

Single Lipoplex Study of Cationic Lipoid-DNA, Self-Assembled Complexes

Edwin V. Pozharski[†] and Robert C. MacDonald^{*}

Department of Biochemistry, Molecular Biology and Cell Biology, Northwestern University, Evanston, Illinois 60208

Received June 13, 2007; Revised Manuscript Received August 3, 2007; Accepted August 24, 2007

Abstract: A flow fluorometric analysis (using a commercial flow cytometer) of individual cationic lipoid-DNA complexes is presented. Such single lipoplex studies have the advantage of providing detailed characterization of heterogeneous ensembles of lipoplex preparations that cannot be obtained with methods that provide only population averages. Specifically, the composition (amount of lipoid and the lipoid-DNA ratio) was determined for statistically large ensembles (10^3 – 10^4 particles) under a variety of conditions, including DNA:lipoid mixing ratio, lipoid dispersion method (extruded, vortexed), DNA morphology (linear, supercoiled), and concentration. In addition, the kinetics of formation were assessed for several conditions. Under essentially all conditions, two distinct regimes were observed, and on the basis of present and past data, these were identified as (1) coexistence of multilamellar lipoplexes and DNA-coated vesicles and (2) highly fused multilamellar complexes. The former outcome is favored by excess of DNA, reduced vesicle size, linear DNA, high concentration, and short incubation times. Fused multilamellar complexes represent the structures of lipoplexes usually used for DNA transfection; these were formed by interaction and breakdown of DNA-coated vesicles. Because the composition of individual lipoplexes could be determined, it was possible to assess how much of the bulk sample heterogeneity originates within individual vesicles and how much is due to differences between lipoplexes.

Keywords: Cationic lipid; transfection; flow fluorometry; EDOPC

Introduction

Cationic lipoids (the molecules are lipid-like but not lipids) are known to form complexes with DNA (lipoplexes) that can deliver genetic material into cell nuclei.^{1–3} Numerous studies of their biological and physicochemical properties have been

conducted over many years; however, the relationship between lipoplex structure and biological activity remains unclear.

The formation of the lipoplex supramolecular complex by mixing cationic lipid with DNA is driven by entropy gain resulting from counterion release and/or macromolecule dehydration.^{4,5} The overall binding free energy per nucleotide is rather small ($\sim kT$),⁶ but since most DNAs incorporated into lipoplexes are quite large and because many charges bind as a unit, the equilibrium overwhelmingly favors formation of the complex (except at very high ionic

* To whom correspondence should be addressed: e-mail macd@northwestern.edu; tel 510 5248961.

[†] Present address: Department of Pharmaceutical Sciences, University of Maryland, Baltimore, MD 21201.

- (1) Felgner, P. L.; Gadek, T. R.; Holm, M.; Roman, R.; Chan, H. W.; Wenz, M.; Northrop, J. P.; Ringold, G. M.; Danielsen, M. Lipofection: a highly efficient, lipid-mediated DNA-transfection procedure. *Proc. Natl. Acad. Sci. U.S.A.* **1987**, *84*, 7413–7417.
- (2) Leventis, R.; Silvius, J. R. Interactions of mammalian cells with lipid dispersions containing novel metabolizable cationic amphiphiles. *Biochim. Biophys. Acta* **1990**, *1023*, 124–132.
- (3) Gao, X.; Huang, L. A novel cationic liposome reagent for efficient transfection of mammalian cells. *Biochem. Biophys. Res. Commun.* **1991**, *179*, 280–285.

- (4) Bruinsma, R. Electrostatics of DNA cationic lipid complexes: isoelectric instability. *Eur. Phys. J. B* **1998**, *4*, 75–88.
- (5) Hirsch-Lerner, D.; Barenholz, Y. Hydration of lipoplexes commonly used in gene delivery: follow-up by laurdan fluorescence changes and quantification by differential scanning calorimetry. *Biochim. Biophys. Acta* **1999**, *1461*, 47–57.
- (6) Pozharski, E.; MacDonald, R. C. Lipoplex thermodynamics: Determination of DNA-cationic lipid interaction energies. *Bioophys. J.* **2003**, *85*, 3969–3978.

strength^{6,7}). The well-established equilibrium (or at least quasi-equilibrium) structure of lipoplexes is a multilamellar sandwich in which lipid bilayers alternate with layers of DNA strands,^{8–13} except in the case of unusual lipoids or where helper lipid is included that favors formation of hexagonal structures containing DNA.^{14–16} At lower resolution, particularly that of electron microscopy, other structures have been described, such as “beads on a string”,¹⁷ a “spaghetti and meatball” array,¹⁸ DNA encapsulated within liposomes,⁹ supramolecular assemblies,¹⁹ and DNA-coated vesicles.²⁰ The relationship between these structures and biological activity of lipoplex is poorly understood even though a variety of physical properties and formulation

(7) Eastman, S. J.; Siegel, C.; Tousignant, J.; Smith, A. E.; Cheng, S. H.; Scheule, R. K. Biophysical characterization of cationic lipid–DNA complexes. *Biochim. Biophys. Acta* **1997**, *1325*, 41–62.

(8) Gustafsson, J.; Arvidson, G.; Karlsson, G.; Almgren, M. Complexes between cationic liposomes and DNA visualized by cryo-TEM. *Biochim. Biophys. Acta* **1995**, *1235*, 305–312.

(9) Templeton, N. S.; Lasic, D. D.; Frederik, P. M.; Strey, H. H.; Roberts, D. D.; Pavlakis, G. N. Improved DNA: liposome complexes for increased systemic delivery and gene expression. *Nat. Biotechnol.* **1997**, *15*, 647–652.

(10) Boukhnikachvili, T.; Aguerre-Chariol, O.; Airiau, M.; Lesieur, S.; Ollivon, M.; Vacus, J. Structure of in-serum transfecting DNA-cationic lipid complexes. *FEBS Lett.* **1997**, *409*, 188–194.

(11) Rädler, J. O.; Koltover, I.; Salditt, T.; Safinya, C. R. Structure of DNA-cationic liposome complexes: DNA intercalation in multilamellar membranes in distinct interhelical packing regimes. *Science* **1997**, *275*, 810–814.

(12) MacDonald, R. C.; Ashley, G. W.; Shida, M. M.; Rakhmanova, V. A.; Tarahovsky, Y. S.; Pantazatos, D. P.; Kennedy, M. T.; Pozharski, E. V.; Baker, K. A.; Jones, R. D.; Rosenzweig, H. S.; Choi, K. L.; Qiu, R.; McIntosh, T. J. Physical and biological properties of cationic triesters of phosphatidylcholine. *Biophys. J.* **1999**, *77*, 2612–2629.

(13) Tranchant, I.; Thompson, B.; Nicolazzi, C.; Mignet, N.; Scherman, D. Physicochemical optimisation of plasmid delivery by cationic lipids. *J. Gene Med.* **2004**, *6*, S24–S35.

(14) Koltover, I.; Salditt, T.; Rädler, J. O.; Safinya, C. R. An inverted hexagonal phase of cationic liposome–DNA complexes related to DNA release and delivery. *Science* **1998**, *281*, 78–81.

(15) Koynova, R.; MacDonald, R. C. Cationic O-ethylphosphatidyl-cholines and their lipoplexes: phase behavior aspects, structural organization and morphology. *Biochim. Biophys. Acta* **2003**, *1613*, 39–48.

(16) May, S.; Ben Shaul, A. Modeling of cationic lipid–DNA complexes. *Curr. Med. Chem.* **2004**, *11*, 151–167.

(17) Felgner, P. L.; Rhodes, G. Gene therapeutics. *Nature (London)* **1991**, *349*, 351–352.

(18) Sternberg, B.; Sorgi, F. L.; Huang, L. New structures in complex formation between DNA and cationic liposomes visualized by freeze-fracture electron microscopy. *FEBS Lett.* **1994**, *356*, 361–366.

(19) Gershon, H.; Ghirlando, R.; Guttman, S. B.; Minsky, A. Mode of formation and structural features of DNA-cationic liposome complexes used for transfection. *Biochemistry* **1993**, *32*, 7143–7151.

(20) Huebner, S.; Battersby, B. J.; Grimm, R.; Cevc, G. Lipid–DNA complex formation: reorganization and rupture of lipid vesicles in the presence of DNA as observed by cryoelectron microscopy. *Biophys. J.* **1999**, *76*, 3158–3166.

(21) Chesnoy, S.; Huang, L. Structure and function of lipid–DNA complexes for gene delivery. *Annu. Rev. Biophys. Biomol. Struct.* **2000**, *29*, 27–47.

(22) Bordi, F.; Cametti, C.; Gili, T.; Gaudino, D.; Sennato, S. Time evolution of the formation of different size cationic liposome-polyelectrolyte complexes. *Bioelectrochemistry* **2003**, *59*, 99–106.

(23) Lai, E.; Van Zanten, J. H. Real time monitoring of lipoplex molar mass, size and density. *J. Controlled Release* **2002**, *82*, 149–158.

(24) Simberg, D.; Danino, D.; Talmon, Y.; Minsky, A.; Ferrari, M. E.; Wheeler, C. J.; Barenholz, Y. Phase behavior, DNA ordering, and size instability of cationic lipoplexes. Relevance to optimal transfection activity. *J. Biol. Chem.* **2001**, *276*, 47453–47459.

(25) Oberle, V.; Bakowsky, U.; Zuhorn, I. S.; Hoekstra, D. Lipoplex formation under equilibrium conditions reveals a three-step mechanism. *Biophys. J.* **2000**, *79*, 1447–1454.

(26) Kennedy, M. T.; Pozharski, E. V.; Rakhmanova, V. A.; MacDonald, R. C. Factors governing the assembly of cationic phospholipid–DNA complexes. *Biophys. J.* **2000**, *78*, 1620–1633.

(27) Zuhorn, I. S.; Bakowsky, U.; Polushkin, E.; Visser, W. H.; Stuart, M. C. A.; Engberts, J. B. F. N.; Hoekstra, D. Nonbilayer phase of lipoplex-membrane mixture determines endosomal escape of genetic cargo and transfection efficiency. *Mol. Ther.* **2005**, *11*, 801–810.

(28) Goncalves, E.; Debs, R. J.; Heath, T. D. The effect of liposome size on the final lipid/DNA ratio of cationic lipoplexes. *Biophys. J.* **2004**, *86*, 1554–1563.

(29) Scarzello, M.; Chupin, V.; Wagenaar, A.; Stuart, M. C. A.; Engberts, J. B. F. N.; Hulst, R. Polymorphism of pyridinium amphiphiles for gene delivery: Influence of ionic strength, helper lipid content, and plasmid DNA complexation. *Biophys. J.* **2005**, *88*, 2104–2113.

(30) Rakhmanova, V. A.; Pozharski, E. V.; MacDonald, R. C. Mechanisms of lipoplex formation: Dependence of the biological properties of Transfection complexes on formulation procedures. *J. Membr. Biol.* **2004**, *200*, 35–45.

(31) Elouahabi, A.; Ruysschaert, J. M. Formation and intracellular trafficking of lipoplexes and polyplexes. *Mol. Ther.* **2005**, *11*, 336–347.

(32) Ewert, K. K.; Ahmad, A.; Evans, H. M.; Safinya, C. R. Cationic lipid–DNA complexes for non-viral gene therapy: relating supramolecular structures to cellular pathways. *Expert Opin. Biol. Ther.* **2005**, *5*, 33–53.

procedures have been investigated. These were comprehensively reviewed a few years ago,²¹ and some of the more recent and relevant investigations on size, structure, serum interactions, and formulation procedures that have appeared since then, including refs.^{22–32}

A central and inherent feature of the cationic lipid–DNA complex is its intrinsic heterogeneity; this is reflected both in the diversity of structures formed and in the broad particle size distributions that are invariably observed. This heterogeneity arises primarily as a consequence of the asymmetry between the two leaflets in lipid vesicle.²⁶ Because of the intrinsic heterogeneity of lipoplexes, it has been difficult to convincingly relate structure to optimal biological activity. To deal with such complexity, a method is needed that provides information on each of the lipoplexes of a statistically valid sample, i.e., a single particle method capable of making assessment of a significant population rapidly.

The technique of flow fluorometry using a commercial flow cytometer is capable of providing information on the

lipid content and composition of *single lipoplex particles*,³³ thus giving a new insight into this heterogeneous liposome-based system. Here we describe what this technique revealed about the kinds of lipoplex particles that exist under a variety of formulation conditions. Two distinct regimes were observed: (1) coexistence of DNA-coated vesicles and lamellar complexes; (2) highly fused lamellar complexes. With time, the former are usually converted to the latter, but the rate of conversion varies enormously and depends upon lipid and DNA morphology, lipid:DNA mixing ratios, concentration, and incubation conditions.

Experimental Methods

Materials. The cationic lipid derivative, dioleoyl-*O*-ethylphosphocholine (EDOPC), triflate salt, was synthesized as described.³⁴ A related synthesis has also been described.³⁵ EDOPC is commercially available as the chloride salt from Avanti Polar Lipids (Alabaster, AL). Plasmid DNA (pCM-VSport- β gal, 7853 bp) was propagated and purified by Bayou Biolabs (Harahan, LA). Linear DNA (herring sperm DNA, sheared; shorter than 2 kbp according to the manufacturer) was from Invitrogen (Carlsbad, CA). Ethidium homodimer-2 (Ethd-2) and BODIPY FL C₁₂-HPC (BODIPY-PC) were purchased from Molecular Probes (Eugene, OR). Routine reagents were from standard sources.

Sample Preparation. To prepare vortexed EDOPC vesicles, an aliquot of EDOPC stock solution in chloroform was mixed with the appropriate amount of the fluorescent label (BODIPY FL C₁₂-HPC) in a glass vial. Bulk solvent was subsequently removed with a gentle stream of argon. The resulting film was then dried under high vacuum for at least an hour and then resuspended in PBS and briefly vortexed. Label incorporation was 3 wt %.

Extrusion of the vortexed EDOPC sample was performed as described for DOPC vesicles³⁶ using Nuclepore filters with 200 nm pores. Cationic lipoids were found to adhere to these polycarbonate filters, resulting in significant loss of material at the concentrations we used (0.2 mg/mL); however, measuring the decrease of the fluorescent label emission intensity in detergent-treated (Triton X-100) samples allowed assessment of lipid loss so that concentrations could be accurately established. (Triton X-100 caused identical enhancement of fluorescence for both extruded and vortexed

vesicles.) The filters exhibited saturation behavior; reuse of the same filter with subsequent portions of lipid suspension improved the yield of extrusion.

Plasmid or linear DNA samples were labeled with Ethd-2 by simply mixing them at a 60 bp/dye ratio and incubating for at least 1 h (typically 4 h). A molecule of Ethd-2 carries four cationic charges, so that about 3% of DNA phosphate group charges are neutralized by labeling. DNA phosphate concentration was established by measuring absorbance at 260 nm, assuming $\epsilon = 6600 \text{ M}^{-1} \text{ cm}^{-1}$.

To prepare cationic lipid-DNA complexes, the component in excess was injected into the other using an air-displacement pipettor. In the case of the 1:1 mixture, both directions of injection were examined, with very similar results. For the kinetics experiments, lipid vesicles and DNA were both at net ionic charge concentrations of 15 μM (in PBS), and the mixing volumes were chosen appropriately to give the desired charge ratio. After adding the second component, the suspension was gently swirled and allowed to incubate at room temperature for durations of 1 min to 2 h, depending upon the experiment.

Flow Fluorometry Data Acquisition. Since the method has been described in detail elsewhere,³³ the procedure will only be outlined here. A FACSCalibur flow cytometer from Becton Dickinson (Franklin Lakes, NJ) equipped with a 488 nm argon ion laser was used. Particles were detected on the basis of emission into the FL1 channel (515–545 nm spectral window, suitable for BODIPY-PC, which emits at 513 nm). The threshold was set to zero, and the photomultiplier voltage was set to the maximum value that produced no events from buffer solution during 1 min of data collection. Sample concentration (dilution to \sim 10–30 nM of pure lipid prevented overcrowding of the detection area) and flow rate were adjusted for an event detection rate lower than 1000 events/s to assure the absence of double events. Normally, data were collected for 1 min or as long as necessary to collect at least 10 000 events.

The FL3 channel (spectral window <650 nm) provided information about the amount of DNA in the particle, since the DNA label, Ethd-2, strongly emits into this channel ($\lambda_{\text{em}} = 624$ nm). BODIPY-PC also contributes some intensity to this channel, which has to be taken into account (see below). Voltage for this channel was always chosen to be high enough to maintain the signal above zero.

Bulk fluorescence (as measured in a conventional fluorometer) of both dyes was invariant upon complex formation.

(33) Pozharski, E. V.; MacDonald, R. C. Analysis of the structure and composition of individual lipoplex particles by flow fluorometry. *Anal. Biochem.* **2005**, *341*, 230–240.

(34) MacDonald, R. C.; Rakhmanova, V. A.; Choi, K. L.; Rosenzweig, H. S.; Lahiri, M. K. O-Ethylphosphatidylcholine: A metabolizable cationic phospholipid which is a serum-compatible DNA transfection Agent. *J. Pharm. Sci.* **1999**, *88*, 896–904.

(35) Solodin, I.; Brown, C. S.; Heath, T. D. Synthesis of phosphotriester cationic phospholipids. Cationic lipids. 2. *Synlett* **1996**, *5*, 457–458.

(36) MacDonald, R. C.; MacDonald, R. I.; Menco, B. P.; Subbarao, N. K.; Takeshita, K.; Hu, L. Small-volume extrusion apparatus for preparation of large unilamellar vesicles. *Biochim. Biophys. Acta* **1991**, *1061*, 297–303.

(37) Fang, Y.; Yang, J. Two-dimensional condensation of DNA molecules on cationic lipid membranes. *J. Phys. Chem. B* **1997**, *101*, 441–449.

(38) Clausen-Schaumann, H.; Gaub, H. E. DNA adsorption to laterally structured charged lipid membranes. *Langmuir* **1999**, *15*, 8246–8251.

(39) Fishman, D. M.; Patterson, G. D. Light scattering studies of supercoiled and nicked DNA. *Biopolymers* **1996**, *38*, 535–552.

(40) Pantazatos, S. P.; MacDonald, R. C. Real-time observation of lipoplex formation and interaction with anionic bilayer vesicles. *J. Membr. Biol.* **2003**, *191*, 99–112.

For some investigations, it was desirable to determine whether the lipoid vesicles had retained their aqueous contents upon interaction with DNA. For this measurement, lipoid vesicles were loaded with the polar tracer, rhodamine–isothiocyanate–dextran. The dye emits predominantly into the FL2 channel. The intensity of an event in the FL2 channel (with proper corrections for contributions of both BODIPY and Ethd-2 into that channel; for calibration procedure, see ref 33) was hence representative of the amount of rhodamine–dextran retained by a given particle.

Calibration Procedure. Two components of the flow cytometer optical system, the FL1 and FL3 channels, were used to obtain information about the amount of lipid and DNA in each particle. The FL1 channel signal is proportional to BODIPY-PC emission, since Ethd-2 does not emit in this spectral region. Thus, we used this channel to detect lipoid-containing particles and determine the relative amount of lipid in the particle, which is proportional to the intensity.

To convert the FL3/FL1 ratio into a DNA:lipoid ratio, their net values were plotted against each other. Linear regression of the “lipoid-excess” part of the curve is used for calibration, since all DNA molecules are associated with lipid when the latter is in excess.³³ The slope of the calibration curve gives the factor for conversion of FL3 channel intensity into DNA amount; the extrapolation to pure lipid (the end point can also be independently assessed) gives the amount of BODIPY emission that carries over into FL3.

The amount of lipid in each particle can be evaluated in absolute units if extruded vesicles are used as a standard since the size of these is quite accurately known. Thus, in the present case, the average vortexed vesicle was determined to contain 6.5 times more lipid than a 200 nm extruded vesicle. This means that the diameter of a vortexed vesicle would be about 500 nm if they are spherical and unilamellar, close to that previously measured by dynamic light scattering,¹² but undoubtedly, some proportion of oligolamellar vesicles must be present. It should be recognized, however, that the relationship between size distributions obtained by the flow fluorometry approach and dynamic light scattering technique is not straightforward because the first is sensitive to the amount of lipid in the particle, while the

second measures physical size and generates distributions on the basis of the contribution of different sized particles to the scattering intensity (itself a complex matter, since scattering intensity depends upon both size and refractive index and the latter depends upon composition and structure).

Data Analysis. Raw data were collected using CellQuest, the software provided with the flow cytometer. Size–stoichiometry distributions were then calculated, with the distribution density being proportional to the amount of lipid in particles of specific type. The calculations were done using specially written scripts in MatLab (MathWorks, Inc., Natick, MA).

Results

The flow fluorometry approach allows detection of individual lipoplex particles and characterization of their lipid and DNA content. For presenting the results of these determinations, the amount of lipid is divided by the amount of lipid in the original vesicle (in the case of vortexed preparations, the mean amount was used), and this value is referred to as “normalized lipid content” or, frequently, just “lipoid content”. Since this parameter gives amount of lipid relative to that in the original vesicle, i.e., how “big” the particles is in terms of its lipid content, it allows assessment of the extent of particle coalescence or fusion.⁴⁶

The second parameter used to describe each lipoplex particle is the stoichiometry, namely the DNA/lipid charge ratio. Knowledge of the stoichiometry allows one to distinguish different kinds of lipoplex structures. Data are presented as size–stoichiometry distributions with the distribution density (as the vertical axis in all the graphs presented here) being proportional to the amount of lipid present in all the particles of a given size and composition.

Kinetic Investigation of Lipoplex Formation. When cationic liposomes (or any form of cationic lipid dispersion) are mixed with DNA, some time is required for the evolution of the final lipoplex structure; at the very minimum, the two components first come together, and after they have made contact, some form of rearrangement occurs. The rearrangement may be minor, such as adjustment of the relative positions of DNA strands, or major, as in the case of rupture and re-formation of vesicles. In order to understand the mechanisms of formation of lipoplexes, we have determined the composition and amount of lipid in individual lipoplexes as a function of time after mixing and until the major structural changes have ceased. The immediately following sections describe the kinetics of lipoplex formation for extruded and vortexed lipid preparations at different li-

- (41) Lei, G. H.; MacDonald, R. C. Lipid bilayer vesicle fusion: Intermediates captured by high-speed microfluorescence spectroscopy. *Biophys. J.* **2003**, *85*, 1585–1599.
- (42) Koltover, I.; Salditt, T.; Safinya, C. R. Phase diagram, stability, and overcharging of lamellar cationic lipid-DNA self-assembled complexes. *Biophys. J.* **1999**, *77*, 915–924.
- (43) Pozharski, E.; MacDonald, R. C. Thermodynamics of cationic lipid-DNA complex formation as studied by isothermal titration calorimetry. *Biophys. J.* **2002**, *83*, 556–565.
- (44) MacDonald, R. C.; Gorbonos, A.; Momsen, M. M.; Brockman, H. L. Surface properties of dioleoyl-sn-glycerol-3-ethylphosphocholine, a cationic phosphatidylcholine transfection agent, alone and in combination with lipids or DNA. *Langmuir* **2006**, *22*, 2770–2779.
- (45) Zabner, J.; Fasbender, A. J.; Moninger, T.; Poellinger, K. A.; Welsh, M. J. Cellular and molecular barriers to gene transfer by a cationic lipid. *J. Biol. Chem.* **1995**, *270*, 18997–19007.

- (46) The nature of the process by which initial DNA–vesicle interactions lead to larger particles (when multilamellar lipoplexes are the final product) is not understood in detail. It may resemble fusion of lipid bilayers, or it could be similar to coalescence of oil droplets. Since we cannot distinguish the possibilities, we use the two terms interchangeably. In any case, liposome rupture, in the sense that the bilayer is torn (whether or not it reseals), is likely to be involved in particle growth.

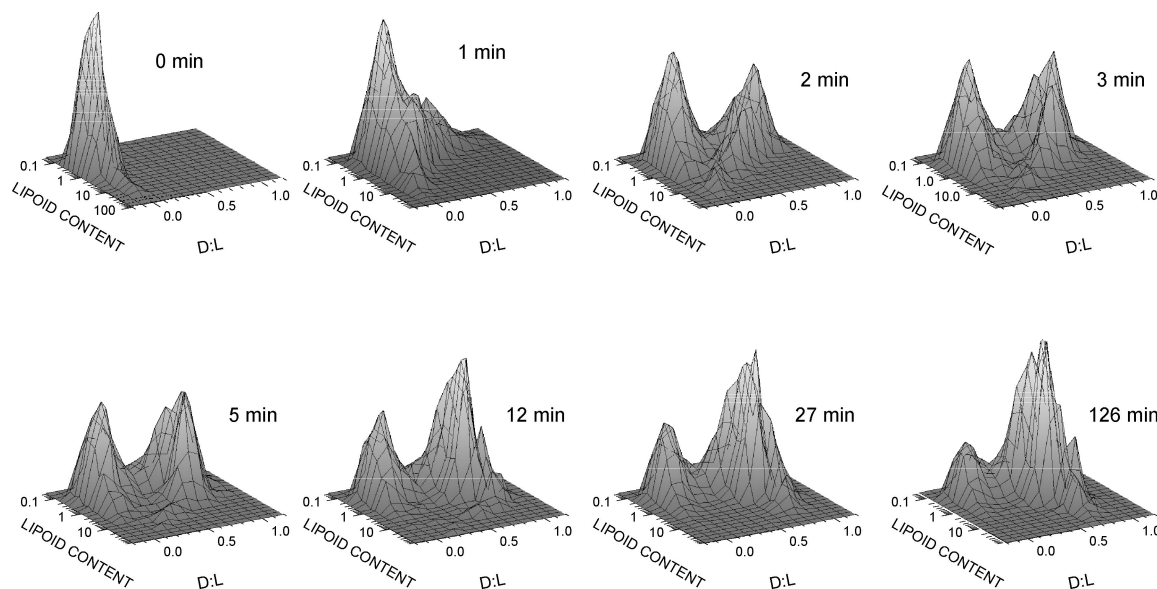


Figure 1. Kinetic investigation of lipoid content–stoichiometry distributions of an equimolar mixture of plasmid DNA and vortexed EDOPC vesicle suspensions. Size is normalized to the average lipoid content of vortexed vesicles in the absence of DNA (upper left panel). Distribution density (vertical axis) represents the amount of lipoid in particles of given stoichiometry and size; thus, in those cases where there are two populations, the relative volume of two peaks represents the ratio of the total amounts of lipoid in two populations. In this and subsequent figures presenting flow fluorometry data, the vertical axis has been set to give about the same vertical projections for all plots; this was done to allow easy assessment of the population distribution within a plot. Otherwise, some plots would be too highly compressed or extended vertically to allow such assessment; however, it means that the relative heights between different plots are not meaningful. Incubation time after mixing is shown next to each panel. DNA concentration was 15 μM (in phosphate) and lipoid concentration was 15 μM .

poid–DNA mixing ratios. For all of the experiments of this section, the DNA and lipoid stock solutions were at 15 μM , and they were mixed in volumes (1:1 or 1:2) to give two different input ratios. These concentrations are lower than those usually used for preparing lipoplexes for cell transfection; however, they were so chosen to ensure that the kinetics were not too fast to be easily resolved by the flow-fluorometric method. It should be recognized that the 1:1 and 2:1 input ratios actually correspond to “DNA-excess” and “lipoid-excess” regimes; as will be seen, this follows from the fact that at an input ratio D:L of ~ 0.7 there is no free DNA, whereas at lower ratios there is free DNA.

Equimolar Lipoid (Vortexed) and DNA. The patterns of evolution of lipoplexes from an equimolar mixture of plasmid DNA and EDOPC prepared by vortexing are shown in Figure 1. The zero-time plot shows the size distribution of the liposomes; these are centered at 0 on the D:L (stoichiometry) axis. After a few minutes incubation in the presence of DNA, a second population began to appear and grow until the distribution consisted of two well-separated particle populations, which we will initially refer to descriptively as “lipoid-rich” and “DNA-rich”. Because the size of the two peaks changes with little change in size or composition, one can conclude that the former population is converted to the latter and that the lifetime of the intermediates must be short relative to the lifetime of the former. As will be seen below, the DNA-rich population corresponds to the

(multi)lamellar complex⁴⁷ that has been well characterized by X-ray diffraction in the case of the lipoid DOTAP¹¹ and more recently for EDOPC.^{12,15} Under these conditions of preparation, an average DNA:lipoid stoichiometry of the complex is about 0.7, as can be seen from D:L axis in the plots for longer incubation times.

The “lipoid-rich” population consists of DNA-coated vesicles, which are known to form upon conditions of DNA excess.^{20,26} (It will become clear below why particles formed under DNA-excess conditions should be lipoid-rich.) We have also established that the input vesicles remain intact because they retain rhodamine–dextran trapped in their aqueous cores (see also ref 33). The average D:L stoichiometry is about 0.1 for the lipoid-rich population generated from vortexed vesicles and is due both to the inaccessibility of inner bilayers of multilamellar vesicles and to the larger spacing of DNA when it is bound to the surface of a monolayer^{37,38} than when it is bound between two monolayers in a lamellar complex.

(47) Although the conditions of preparation for the samples of this investigation were not necessarily the same as for those that had been previously characterized by X-ray diffraction, the latter technique consistently revealed DNA–lipoid multilamellar structures for the (quasi)equilibrium state of EDOPC. In the case of coated vesicles, there is electron microscope evidence for their existence in the case of DOTAP²⁰ and other physical evidence for their existence in the case of EDOPC.^{26,33}

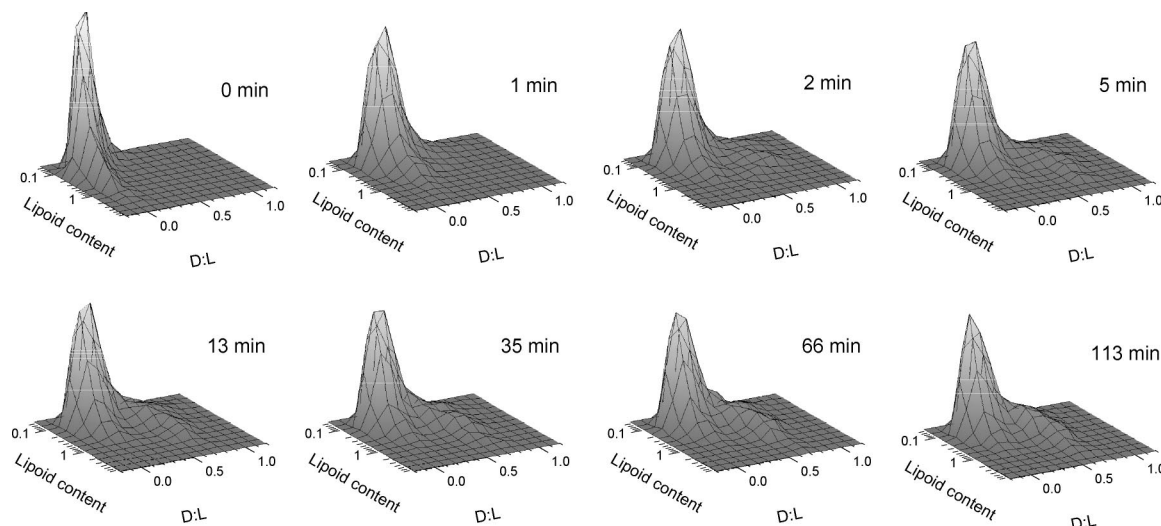


Figure 2. Kinetic investigation of lipoid content–stoichiometry distributions of an equimolar mixture of plasmid DNA and 200 nm extruded EDOPC vesicles. Size is normalized to the average lipoid content of vortexed vesicles (see Figure 1). DNA concentration was 15 μ M (in phosphate) and lipoid concentration was 15 μ M.

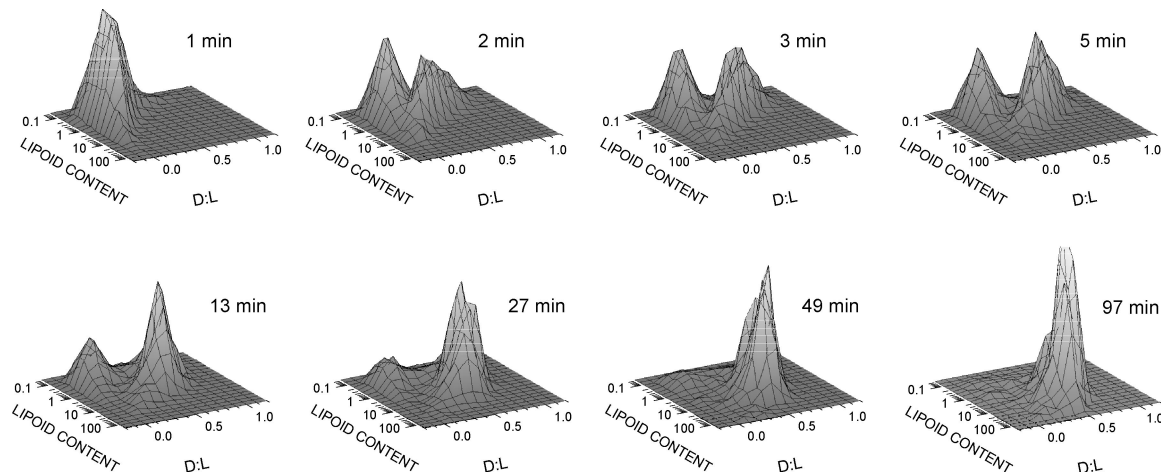


Figure 3. Kinetic investigation of lipoid content–stoichiometry distributions of a 1:2 molar mixture of plasmid DNA and vortexed EDOPC vesicles. Concentrations were 10 μ M for DNA and 20 μ M for vortexed EDOPC. For the distribution density of pure vortexed lipoid, see left upper panel in Figure 1.

Immediately after mixing, most of the lipoid was already in the form of lipoid-rich particles, having adsorbed enough DNA to cover the available liposome surface (see panel “1 min” in Figure 1, where the peak shifts to $D:L = 0.1$ from a value of 0.0 at 0 min). These structures were subsequently transformed into DNA-rich particles, with the final stoichiometry being reached after 10 min of incubation, following which time some limited coalescence occurred. This coalescence can be appreciated from Figure 5 (first plot, upper left), which presents the mean stoichiometry and the lipoid content relative to the mean lipoid content of the original vesicles (“degree of fusion”), both of which are given as a function of time for the lipoplex population as a whole; i.e., it presents the composition and growth of particles as it would be measured by a population averaging technique. About 20% of the lipoid remained in form of lipoid-rich particles even after prolonged (>2 h) incubation, and this

stable population consisted of particles that contained about 5 times less lipoid than average vesicle presented in original vortexed lipoid preparation.

Lipoid (Vortexed) in Excess Relative to DNA. In contrast to lipoplex formation from vortexed lipoid when lipoid and DNA were equimolar (Figure 1), when lipoid was in excess, essentially all lipoid and DNA became converted to lamellar complex (Figure 3). For perhaps the first 10–15 min, the processes were similar for the two input ratios, but at a 1:1 input ratio, there was little subsequent change, whereas when input lipoid was in excess, DNA-coated vesicles continued to disappear into condensed lipoplexes until, by an hour, coated vesicles were essentially eliminated.

As shown in Figure 5, the final mean stoichiometry in this situation ($D:L = 0.5$) matches the DNA:lipoid mixing ratio, showing that all the DNA was complexed with lipoid. The uptake of DNA took about 3 times longer than in the case of

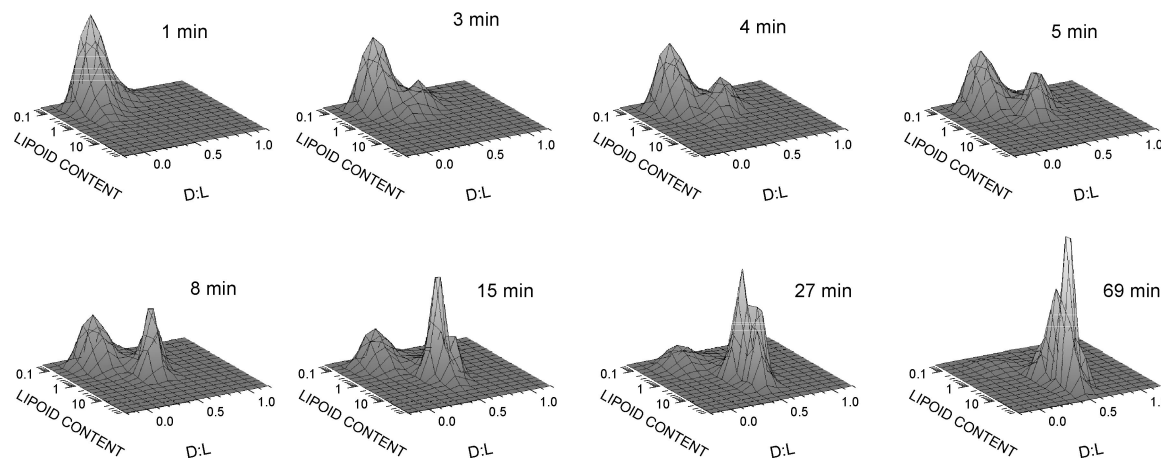


Figure 4. Kinetic investigation of lipoid content–stoichiometry distributions of a 1:2 molar mixture of plasmid DNA and 200 nm extruded EDOPC vesicles. Size is normalized to the average lipoid content of vortexed vesicles (see Figure 1). DNA concentration was 15 μ M (in phosphate) and lipoid concentration was 15 μ M.

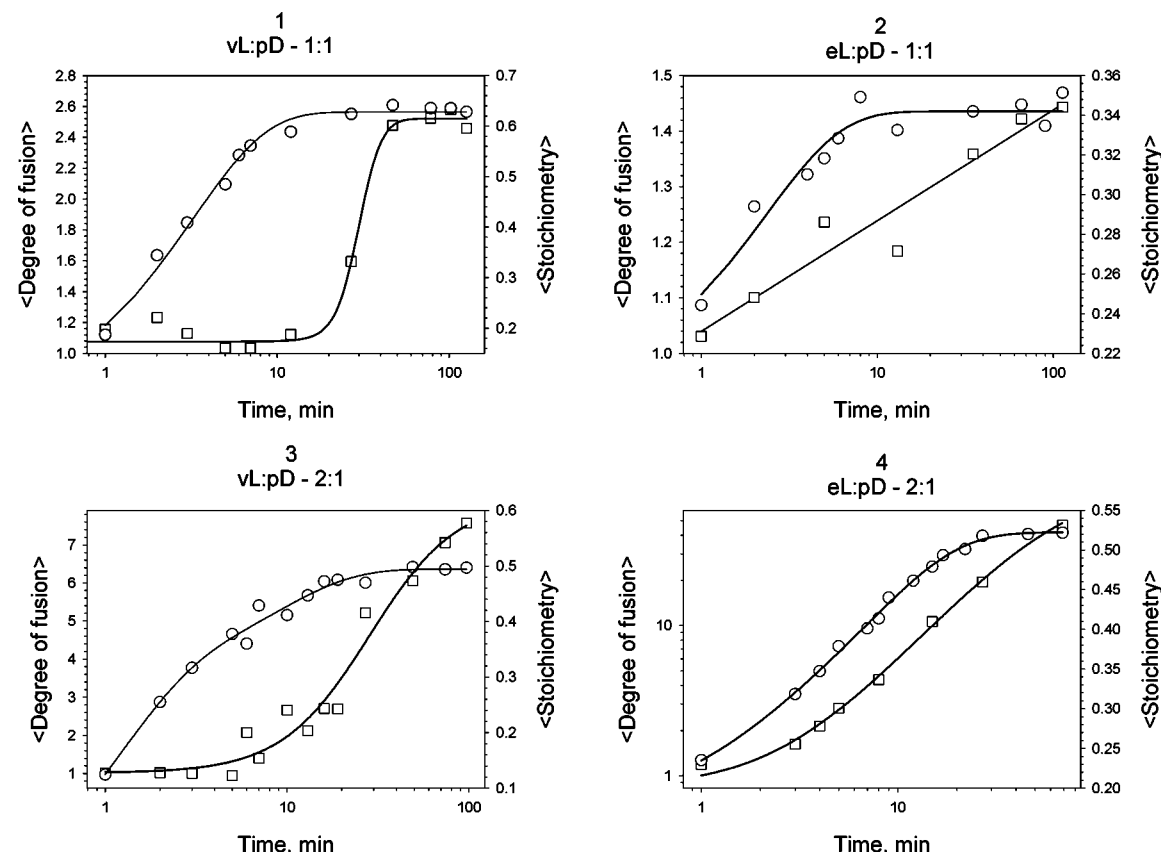


Figure 5. Average DNA:lipoid stoichiometry and degree of “vesicle fusion” of lipoplexes versus incubation time. The degree of vesicle fusion (squares) is the average number of vesicles (extruded or vortexed) that coalesced to form an average lipoplex particle after the duration of incubation shown. Stoichiometry is represented by circles; the mean values presented here correspond to those that would be found by a population averaging technique. The four panels correspond to Figures 1–4.

the equimolar mixtures. No coalescence or fusion (i.e., growth) occurred within the first several minutes of incubation, but then at about 5 min, the average particle size began to increase steadily, so that at the end of the experiment (1.5 h of incubation, see Figure 5), lipoplex particles contained an amount of lipoid corresponding to that of about eight original vesicles.

Equimolar Lipoid (Extruded) and DNA. The dependence of lipoplex structure on vesicle size is illustrated in Figure 2, wherein the evolution of lipoplexes formed from extruded vesicles is shown. The size is normalized to the average size (amount of lipoid in the average particle) in the *vortexed* lipoid preparation, and it is clear that the

particles stably coated with DNA in Figure 1 correspond approximately in size to the extruded vesicles of Figure 2 (note that a logarithmic scale is used for lipid content). It is evident that not very much of the DNA-rich population formed even after prolonged incubation; in this case, 80% of the lipid remained in lipid-rich particles, even after 2 h incubation. As shown in the second plot of Figure 5, the entire extent of DNA uptake occurred within first 10 min of incubation, and the only subsequent change was a slow but steady coalescence leading to growth of particles.

Similarly to the situation with vortexed lipid, vesicles became coated with DNA immediately upon mixing. (The “1 min” plot in Figure 2 shows the peak shifts to $D:L = 0.25$ from 0 at zero time.) Nevertheless, the average stoichiometry of the DNA-coated vesicles was higher than with vortexed lipid because of the absence of multilamellar vesicles that contain inaccessible lipid (which is thus necessarily suprastoichiometric) buried in inner bilayers.

Lipid (Extruded) in Excess Relative to DNA. As in the case of lipoplex formation from vortexed lipid in excess, when extruded lipid was in excess, the entire amount of lipid was eventually converted to DNA-rich particles. This is illustrated in Figure 4.⁴⁸ Two distinct populations were observed, with condensed lipoplexes becoming more plentiful at the expense of DNA-coated vesicles until, as shown in the relevant panel of the figure, after an hour essentially only condensed multilamellar lipoplexes were present. The entire time progression of particle size and stoichiometry change are given in Figure 5 (plot 4, lower right), where it can be seen that almost no lag in coalescence was detected under these conditions (in contrast to excess vortexed lipid, shown in plot 3, lower left), perhaps because the concentration of vesicles (not lipid) is higher in the extruded preparations.

Effect of DNA:Lipid Mixing Ratio under Typical Lipoplex Formation Conditions. For experiments described here and subsequently, “standard conditions” represent vortexed lipid and plasmid DNA mixed at a total concentration of $100 \mu\text{M}$. This was done because such conditions are similar to those commonly used for lipoplex preparation in biological applications. Under these conditions, the set of lipid content–stoichiometry distributions obtained 1 h after mixing (at which time size and composition have stabilized) for different DNA:lipid mixing ratios is shown in Figure 6. These data clearly illustrate the change of the structural outcome regime from that of coexistence of DNA-coated vesicles (toward the left side of the $D:L$ axis in the 1:1, 2:1, 4:1 and 8:1 plots) to that of highly fused lamellar complexes (in the region of 0.5 on the $D:L$ axis) as the DNA:lipid mixing ratio was changed from DNA excess to lipid excess.

At a DNA:lipid mixing ratio of about 1:2, there was a rather pure and relatively homogeneous population of li-

poplexes, whereas at higher lipid excess, coated MLV’s (multilamellar vesicles) as well as a small amount of lipid vesicles with no associated DNA became evident (Figure 6). Similarly, at a DNA:lipid mixing ratio of about 1:2 there was no free DNA, but as the DNA concentration was increased, DNA-coated vesicles began to become prevalent (Figure 6), and on the basis of other results, free (unbound) DNA would begin to appear in solution.³³

As is evident from Figure 6, the average stoichiometry of plasmid DNA-coated vortexed lipid vesicles is about 0.05–0.15, whereas the stoichiometry of lamellar lipoplexes is 0.65–0.75 when they coexist with DNA-coated vesicles. (Otherwise, the stoichiometry of lamellar lipoplexes matched the DNA:lipid mixing ratio.)

The average lipid content of lipoplex particles as a function of the mixing ratio is shown in Figure 7. There was almost no fusion or coalescence when DNA was in excess; under these conditions single lipid vesicles were transformed into single lipoplex particles. On the other hand, when $D:L < 1$, there was considerable coalescence of lipid vesicles as they interacted with DNA, and the result was a broad maximum in the distribution at around $D:L \sim 0.5$. At the maximum, about 11 original vesicles on average formed a final lipoplex particle. This level of coalescence strongly depended upon concentration, decreasing with dilution (Figure 9). Less coalescence also occurred at large lipid excesses.

The amount of free DNA per unit of lipid in samples with different mixing ratios can be determined from the difference between the expected and the actual emission of the DNA label, summed over the whole population of detected particles. (Whatever fraction of the DNA label that is “missing” corresponds to that not associated with lipoplexes, for DNA in solution was not detectable.) As pointed out elsewhere,³³ and shown below (see Discussion), all of the DNA present is associated with lipid unless the $D:L$ mixing ratio exceeds a critical value of about 0.7. For $D:L > 0.9$, the amount of free DNA increases linearly with a slope close to unity.³³

Effect of DNA Morphology: Plasmid versus Linear DNA. Although there are distinct quantitative differences, qualitatively, lipoplexes formed by linear DNA exhibit the same structural behavior as those formed with plasmid DNA. Similarities and differences between these two cases are summarized below, and the corresponding data are presented in Figure 8.

(1) At concentrations typical for gene delivery ($100 \mu\text{M}$, total), linear DNA or plasmid DNA both gave rise to DNA-coated vesicles coexisting with lamellar lipoplexes under DNA-excess conditions and to highly fused lamellar lipoplexes under lipid-excess conditions (Figure 9, first row, first and second columns).

(2) DNA-coated vesicles are significantly more stable (i.e., fewer lamellar lipoplexes formed) when linear DNA was used (first row, first and second columns of Figure 8).

(3) Lamellar lipoplexes incorporated significantly more linear than plasmid DNA. When DNA-coated vesicles

(48) Six of the plots of this figure were published previously (Pozharski and MacDonald, 2005). Those data are reproduced here with permission of Elsevier.

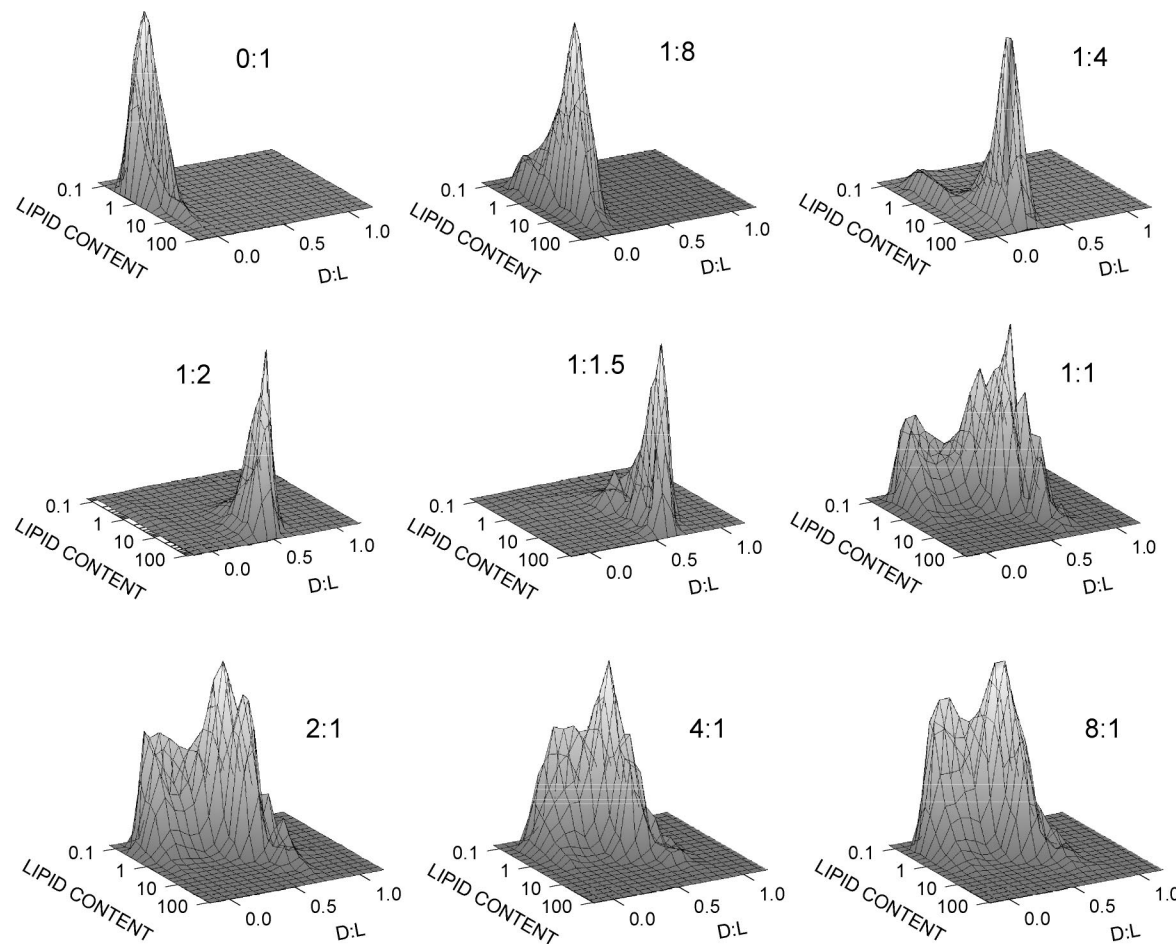


Figure 6. Lipoid content–stoichiometry distributions of vortaxed EDOPC mixtures mixed with plasmid DNA at different mixing ratios. The sum of lipoid and DNA concentrations was $100 \mu\text{M}$ in all samples, and incubation was for an hour prior to data collection. Numbers over the plots are the D:L mixing ratios (molar charge).

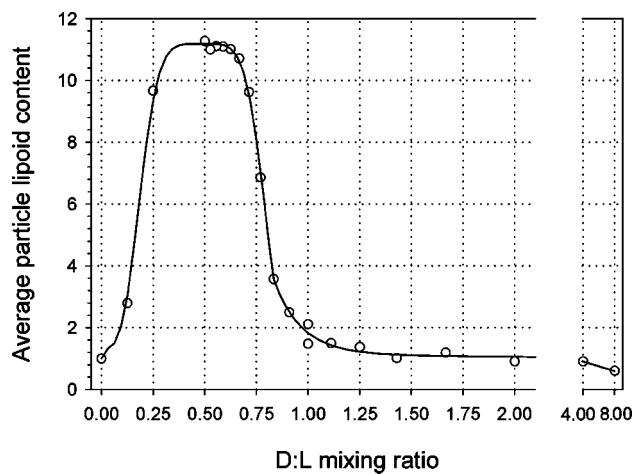


Figure 7. Mean number of vortaxed vesicles coalescing to form the average lipoplex particle at different mixing ratios. These data were derived from those of Figure 5; conditions are given in the legend to that figure.

coexisted with lamellar lipoplexes, the stoichiometry of the latter was about 0.7 in the case of plasmid DNA, whereas it increased to about 0.9 in the case of linear DNA (first row, first and second columns, Figure 8).

(4) When lipoid was in excess, the structural outcome was independent of DNA type (second row, first and second columns, Figure 8), except that the lipoplexes formed from linear DNA were more heterogeneous with respect to both lipoid content and composition, perhaps reflecting the greater heterogeneity of the linear DNA preparation we used. In the cases of both linear and plasmid DNA, highly fused lipoplexes formed, and the extent of such coalescence was practically the same, given concentrations that were the same. The stoichiometry of the resulting lipoplexes was again found to match the DNA:lipoid mixing ratio.

Effect of Concentration. Total (lipoid plus DNA) concentrations from about 3 to $100 \mu\text{M}$ were examined. It was found that decreasing concentrations had pronounced effects on both coated vesicle and condensed lipoplex regimes.

An interesting feature of low-concentration samples is illustrated in the first and third plots in the lower row of Figure 8, where the lipoid content–stoichiometry distributions of lipoid-excess samples are shown for high and low concentration samples, respectively. In addition to the shift to smaller lipoid contents, the distribution for the low concentration sample exhibits a strong dependence of stoichiometry on lipoid content, which varies from 0.75 for the

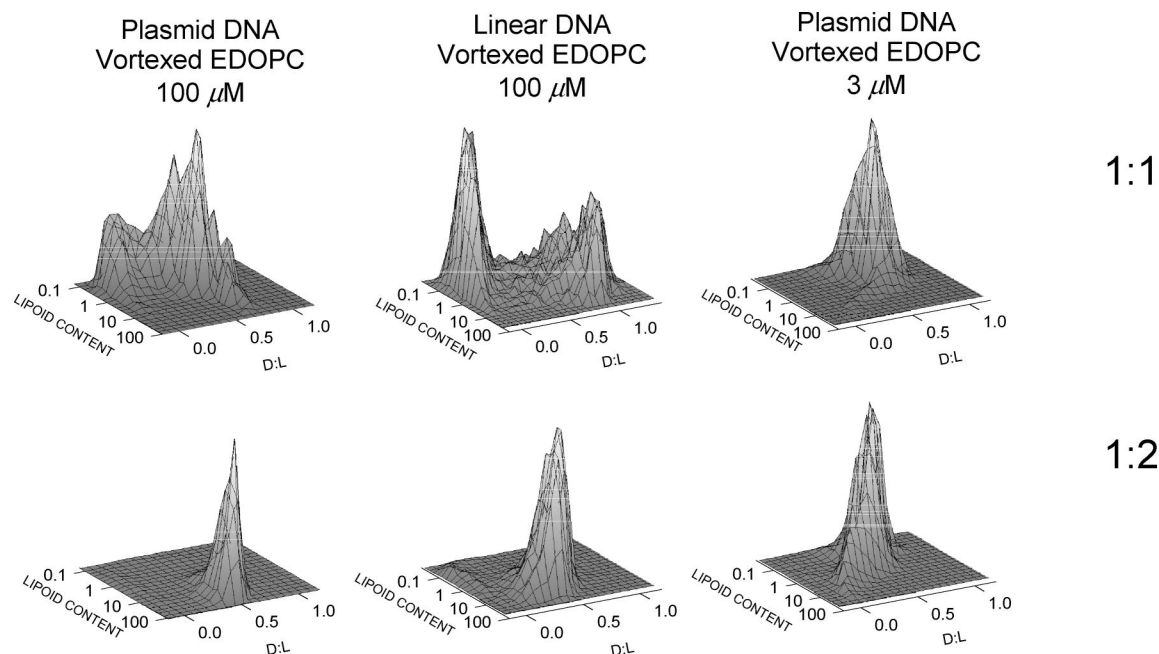


Figure 8. Lipoid content–stoichiometry distributions of different lipoplex preparations: influence of DNA morphology and total concentration. Upper row corresponds to equimolar mixtures. Lower row corresponds to twice (molar ratio) as much lipoid as DNA. Columns are (1) plasmid DNA + vortexed lipoid, 100 μ M total concentration; (2) linear DNA + vortexed lipoid, 100 μ M total concentration; and (3) plasmid DNA + vortexed lipoid, 3 μ M total concentration. Samples were incubated for an hour before collecting data. The effect of DNA type is seen by comparing column 1 with column 2, and the effect of total concentration is seen by comparing column 1 with column 3.

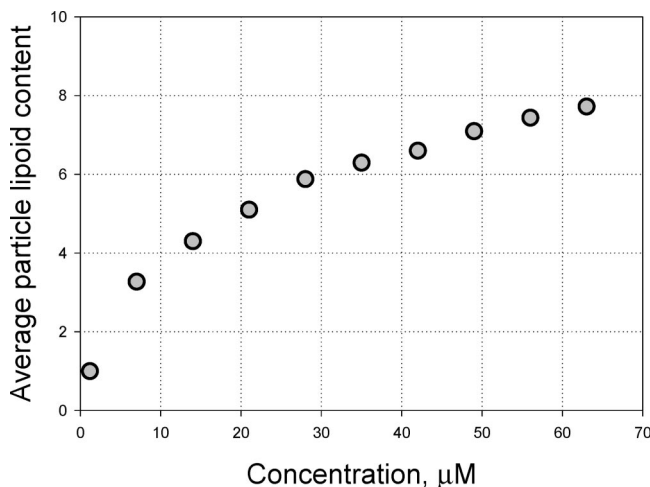


Figure 9. Average lipoid content of lipoplex particles (normalized to the mean lipoid content of vesicles) versus total EDOPC and DNA concentration at a 1:5 DNA to lipoid mixing ratio (molar). The first point represents pure lipoid at 1.2 μ M. Samples were incubated for an hour.

smallest particles to 0.25 for the largest in this preparation in which lipoid was in 2-fold excess.

Reducing input concentrations resulted in dramatic changes of structural outcomes in the case of equimolar mixing stoichiometry. When the complex concentration was below 10 μ M, only fused lamellar lipoplexes formed and coexisting DNA-coated vesicles were not present (see Figure 8, upper row, first and third plots). Interestingly, the degree of fusion was approximately the same for both 1:1 and 1:2 mixing ratios.

When lipoid was in excess, fused lamellar complexes formed at all concentrations; however, the degree of fusion or, equivalently, particle size (expressed as the average amount of lipoid in the lipoplex particle relative to that of original vesicle) increased monotonically with increasing concentrations. This behavior is shown in Figure 9, for which the input ratio D:L was 1:5, and the concentration is the sum of the concentrations of DNA and lipoid. Over this range of concentration, the particle size, as measured by average lipoid content, changed by about an order of magnitude, from that of a single vesicle to that of eight vesicles.

Discussion

Condition-dependent differences in lipoplex structure may be attributed to the *intrinsic asymmetry of lipoid vesicles*.²⁶ In particular, the inner leaflet of the bilayer is not immediately accessible to DNA, and vesicle rupture is required to convert a vesicle into a multilamellar lipoplex. There are two principal structural outcomes for cationic lipid–DNA complex preparations: (1) coexistence of DNA-coated vesicles with multilamellar lipoplexes and (2) highly fused multilamellar lipoplexes. These outcomes are readily rationalized on the basis of the following considerations: Upon mixing, cationic lipid and DNA quickly bind to each other. When DNA is in excess (at least relative to *exposed* lipid), it coats vesicles, and this structure is stable only when free DNA is present. Excess DNA is necessary for uniform coating, which probably stabilizes vesicles through two mechanisms: (1) with incomplete coating, nonuniform stresses are created along the surface of the vesicle; (2) vesicles with patches of

positive and negative surface charge adhere, which also generates stress. Both of these effects can cause rupture. Broken vesicles acquire additional DNA (if available) and form multilamellar lipoplexes; these can then, in turn, coalesce either with other multilamellar lipoplexes or with DNA-coated vesicles, inducing the rupture of the latter. Thus, when equilibrium is eventually attained, only the multilayer structure is present. Because full equilibration is not normally included in protocols for biological applications of lipoplexes, intermediate structures may influence the biological activity of these gene delivery agents.

Kinetic Considerations of Lipoplex Formation. Lipoplex Formation Depends on Competition between Vesicle Rupture and Coating by DNA. Provided DNA is in excess, DNA-coated vesicles can be stable for hours.^{20,26} The critical period when vesicle rupture could occur is the short time before complete coating. It is evident, then, that competition between vesicle rupture and vesicle coating determines the amount of lipoid that becomes multilamellar lipoplex. We next estimate the rates of both processes.

There has been some prior examination of the kinetics of lipoplex formation.^{22,23} Importantly, these studies recognized two basic classes of particles under most formation conditions; however, they utilized dynamic light scattering of whole populations and so could not provide data on microscopic initial steps. It is almost certain that binding itself is very fast so that the DNA-lipoid surface interaction is diffusion-controlled, and we calculate that, for the average MLV in a vortexed preparation, the coating time, τ_c , is ~ 300 ms.⁴⁹

Rupture rates cannot be calculated from fundamental principles, but there is good indication that they can be fairly high. Interaction of giant cationic lipoid vesicles with DNA surfaces, as observed by fluorescent microscopy, revealed that one mode of interaction was rupture,⁴⁰ and when that

(49) Bimolecular rate constants for diffusion-controlled reactions (in $M^{-1} s^{-1}$) are given by $k = 4\pi r_0(D_A + D_B)10^{-3}N_0$, where r_0 is the closest approach distance between reactants (in cm), D_A and D_B are their diffusion coefficients (in cm^2/s), and N_0 is Avogadro's number. Using literature data,³⁹ we estimate the radius of gyration of pCMV Sport- β gal plasmid DNA as ~ 100 nm and the diffusion coefficient as $\sim 3 \times 10^{-8} \text{ cm}^2/\text{s}$. The average diameter of vortexed EDOPC vesicles is about 500 nm, and the diffusion coefficient is $\sim 5 \times 10^{-8} \text{ cm}^2/\text{s}$ (determined by dynamic light scattering). Hence, $r_0 \sim 3.5 \times 10^{-5} \text{ cm}$, $(D_A + D_B) \sim 8 \times 10^{-8} \text{ cm}^2/\text{s}$, and $k \sim 2 \times 10^{10} M^{-1} s^{-1}$ (concentrations are in plasmids and vesicles per unit volume). "Coating time" τ_c is about $N/k[pDNA]_0$, where $[pDNA]_0$ is initial concentration of plasmid DNA molecules and N is the number of plasmids binding to a single vesicle. For typical conditions used for laboratory preparation of lipoplexes (60 μM plasmid DNA mixed with 30 μM vortexed lipoid), $\tau_c \sim 12N$ ms. We found that the D:L stoichiometry of DNA-coated extruded vesicles is about 0.2. Hence, 0.4 DNA charges bind to one lipoid charge at the outer surface of the average vesicle. For $D_v = 500$ nm diameter vesicles and 7853 bp long plasmid DNA ($N_p = 15\,706$ negative charges per DNA molecule) this gives $N \sim (0.4\pi D_v^2)/(S_L N_p) \sim (0.4 \times 3.14 \times 2.5 \times 10^7 \text{ \AA}^2)/77 \text{ \AA}^2 \sim 26$ plasmid DNA molecules to cover an average MLV. The final estimate of the coating time is then $\tau_c \sim 300$ ms.

occurred, it did so in one or two video frames, i.e., corresponding to $\tau_r \sim 30\text{--}60$ ms. Given the conditions and the DNA-coating time estimate from above, a substantial proportion of lipoid would be converted into multilamellar lipoplexes, as we observed experimentally.

Extruded Vesicles Form More Stable Coated Vesicles Than Do Larger Vesicles. When extruded (200 nm) EDOPC vesicles were mixed with plasmid DNA in equimolar amounts, DNA-coated vesicles formed rapidly, with the D:L stoichiometry of most of the population changing to almost 0.2 (relative to 0.0 for the vesicles alone) within the first minute after mixing (Figure 2). Similarly, vortexed MLVs also acquired a DNA coating within the first minute, but the stoichiometry of the initial population was 0.1, reflecting the larger proportion of lipoid in internal layers (Figure 1). The rate of coating of the small vesicles is expected to be higher than that of the larger vesicles,⁵⁰ but the difference may not have been apparent, since at the concentrations we used a minimum of about 1 min was necessary for data collection. In any case, the most dramatic difference between the two experiments is that the coated extruded vesicles remain intact to a large extent for the duration of the experiment (113 min), whereas the vortexed preparation was largely converted to multilamellar lipoplexes having a D:L of 0.7. Indeed, within 5 min, half of the lipoid in the vortexed preparation became lipoplexes, and the process of fusion to generate larger lipoplexes was already detectable at 1 min. These results are consistent with previous titration experiments in which we measured the release of contents (based on fluorescence from a terbium ion chelate) from vortexed and extruded preparations upon contact with DNA.³⁰

What accounts for this difference in stability of the large and small vesicles? As mentioned, the small vesicles should be coated faster than larger vesicles. The one additional difference we can identify that could contribute to the difference in conversion to lipoplexes has to do with stability upon contact with an oppositely charged surface. The largest mechanical stress in these systems is likely to come from adhesion of vesicles mediated by DNA, as comes about when a DNA-coated lipoid surface contacts DNA-free lipoid surface and the two surfaces are drawn together to maximize adhesion area; this causes mutual flattening of the two bilayer surfaces and stretching of the whole shell of the vesicle which, if continued, leads to rupture (similar to the rupture induced by mutual adhesion of cationic and anionic vesicles).⁴¹ The energy of such interactions would be larger, the larger and less curved are the participating vesicles. Furthermore, such asymmetric forces are likely to be much more disruptive than the isotropic forces operating on an isolated vesicle uniformly coated with a layer of DNA, especially if the vesicle is small and the DNA is relatively

(50) The smaller vesicles diffuse faster but have a smaller collision cross section; the result is that these two factors very nearly cancel out. However, another factor is that the amount of DNA needed to cover the vesicle surface is proportional to surface area, or D_v^2 . As a result, the coating time τ_c is ~ 50 ms for extruded vesicles.

weakly bound. Although we did not incubate for short enough times to establish a difference between coating of small and large vesicles, given their higher volume to surface ratio, extruded preparations are expected to retain a fluorescent marker longer than vortexed preparations. Thus, it seems likely not only that the small vesicles are more rapidly protected by a coat of DNA which discourages adhesion with others of their kind but also that they are also more stable to rupture.

Decreasing concentrations favor multilamellar lipoplexes by slowing coating of the lipid with DNA, e.g., the difference ($\sim 30\times$) in concentrations for the experiments of Figure 9 (first row, compare columns 1 and 3) would increase the coating time to as long as 1.5 s, even for smaller vesicles and unquestionably provide more time for vesicle rupture. Additional experiments like those of Figure 9 showed that DNA-coated vesicles are essentially absent when plasmid DNA concentration was below $\sim 15\ \mu\text{M}$ (corresponding to $\tau_c \sim 200\ \text{ms}$). This was also true in the case of extruded vesicles.

In addition to lowering the concentrations of lipid and/or DNA, another way to favor conversion of coated vesicles to multilamellar lipoplexes is to use a multistep formulation procedure (titrating DNA into lipid to assure local lipid excess) instead of one-shot mixing. Such procedures and their outcomes with respect to physical properties²⁶ and transfection activity³⁰ have been described.

A Higher Concentration of Lipid Relative to DNA Leads to More Extensive Vesicle Disruption. When the input molar ratio favored lipid over DNA by a factor of 2, both extruded and vortexed lipid vesicles formed highly fused lamellar lipoplexes with DNA, and in both cases, their stoichiometry matched the DNA:lipid mixing ratio. In the case of the vortexed vesicles, the largest effect of increasing the lipid excess was to reduce the lifetime of the coated vesicles. The latter persisted for more than an hour at a 1:1 input ratio but had largely disappeared within a half hour when the lipid concentration was twice that of the DNA (compare Figures 1 and 3). In the case of extruded vesicles, the effect of increasing lipid concentration was quite dramatic; when DNA and lipid concentrations were the same, coated vesicles were the predominant particles present after an hour, whereas when the lipid concentration was double that of the DNA, coated vesicles were completely replaced by lipoplexes after the same incubation time (compare Figures 2 and 4).

As shown in the first five panels of Figure 6 (for a set of summary data covering a wider range of concentrations, see Figure 2 of ref 33), when lipid is in excess relative to DNA, the resultant lipoplexes have a composition that is equal to the mixing ratio, at least for mixing ratios as high as 32 mol of lipid charge per mole of DNA charge (not shown, but the highest tested). In contrast to these results that show that considerable excess lipid relative to DNA is incorporated into lipoplexes generated by mixing, the incorporation of excess lipid from liposomes into preformed lipoplexes is

very slow. This was clearly revealed by forming complexes with D:L = 1:4 and then adding an equal amount of cationic lipid. Although not studied over long times of incubation, the result was a mixture of the 1:4 lipoplexes and separate cationic liposomes (data not shown). There are very substantial kinetic constraints on these systems, and it is not yet clear how true equilibrium states can be established.

Overcharging in lipoplexes (formation of complexes having an excess of one charged component over the other) has been extensively studied by others,^{4,42} and the driving force was proposed to be the entropy gain upon release of counterions *within* the lipoplex.

The conversion of input vesicles to lipoplexes and the match of the stoichiometry of the lipoplexes to the input ratio of DNA and lipid are evidently a reflection of the same set of processes involving extensive aggregation and vesicle disruption. Why are these processes so much more extensive when the DNA to lipid input ratio is 1:2 (or lower) than when it is 1:1? An important issue, as we have already seen, is how quickly and extensively the lipid is coated with DNA, with rapid and complete coating giving rise to particles that are relatively inert to further interactions. Even at the 1:1 input ratio, the amount of DNA exceeds that necessary to interact with the lipid surface because much (half in the case of extruded vesicles, considerably more than half in the case of vortexed vesicles) is internal and inaccessible. When lipid concentrations are increased, the chances of coating the outsides of vesicles decrease and the likelihood of exposed lipid increases.⁵¹ This increases the chances that adhesion of two or more vesicles may be mediated by the same DNA molecules, a situation that generates high stresses and is likely to induce vesicle rupture. Rupture, in turn, exposes additional lipid to the free DNA in solution until the latter is exhausted.

Of interest is that the average absolute lipid content (not normalized to the lipid content of original vesicle) of the final lipoplexes was approximately the same for both extruded and vortexed vesicles when input lipid was in excess. This means that, in both preparations, fusion to the same size end particle occurred but that more extruded than multilamellar vesicles came together to form a mature lipoplex particle. What accounts for this convergence of sizes is not obvious.

(51) At minimum, formation of coated vesicles requires excess DNA molecules in bulk solution. Given the stoichiometries we determined for DNA-coated vesicles and multilamellar lipoplexes, this condition fails when more than 2/3 of lipid in vortexed preparations has been converted to multilamellar lipoplexes in the case of vortexed lipids at a 1:2 molar input ratio of DNA to lipid. This can be understood as follows: If α is the fractional amount of lipid in the lipid-rich population (representing multilamellar lipoplexes), then $1-\alpha$ is the fractional amount of lipid in the DNA-rich population (representing coated vesicles). Fractions of DNA in both populations are 0.1α and $0.7(1-\alpha)$. It follows therefore that at DNA:lipid mixing ratio ρ , the amount of free DNA, β , is given by $\beta = \rho - 0.1\alpha - 0.7(1-\alpha)$. To satisfy $\beta > 0$, i.e., the presence of free DNA, then $\alpha > (0.7-\rho)/0.6$. When $\rho = 0.5$, this gives $\alpha > 1/3$.

Structural Aspects of Lipoplex Preparations. Stoichiometry of DNA-Coated Vesicles. In DNA-coated vesicles, a layer of DNA strands (more or less parallel)²⁰ covers a lipoid bilayer. In multilamellar lipoplexes, the same arrangement occurs, except that it is repeated a number of times to generate a stack. Since the same basic structure appears in both DNA-coated vesicles and multilamellar lipoplexes, a substantial contribution to the difference in their apparent stoichiometry (~0.2 and ~0.7, respectively, corresponding to about 5 and 18 plasmids per vesicle, respectively) must be a consequence of the difference in DNA spacing, with the larger amount of DNA in the lipoplexes being more closely packed (within limits, until strand–strand repulsion prevents smaller separation). Indeed, the plasmid DNA spacing observed in multilamellar complexes of the composition described here is 31–32 Å,¹⁵ whereas for surface-bound DNA it is 40–60 Å,^{37,38} as would be the case for DNA-coated vesicles. A single lipoid surface cannot compensate for DNA–DNA repulsion at small spacings because DNA strands that adsorb on the surface provide less entropy gain (fewer counterions and water molecules are released), which is the driving process that provides the driving force for lipoplex formation.^{4,5} Thus, DNA–DNA repulsion (the major component of the endothermic binding enthalpy⁴³) leads to the increase of spacing in coated vesicles.

Stoichiometry of Multilamellar Lipoplexes. The DNA:lipoid charge ratio in multilamellar complexes is equal to S_L/S_D , where S_L is the area per lipoid molecule in a bilayer and S_D is the projected area per base pair of a DNA molecule. Monolayer techniques have indicated that, for EDOPC, S_L is about 70 Å² (at 35 mN/m).⁴⁴ S_D can be estimated as dl_{bp} , where d is DNA spacing and $l_{bp} = 3.5$ Å is the DNA double-strand length per base pair. Hence, $D:L \sim 70 \text{ Å}^2/d \cdot 3.5 \text{ Å} = 20 \text{ Å}/d$.

When multilamellar complexes are formed from an excess of DNA over lipoid, the stoichiometry is, according to our data, $D:L \sim 0.9$ for linear and $D:L \sim 0.7$ for plasmid DNA, which correspond to DNA spacings of $d \sim 20 \text{ Å}/0.9 \sim 22 \text{ Å}$ and $d \sim 31 \text{ Å}$, respectively. The latter is in excellent agreement with X-ray analyses of EDOPC lipoplex structure, which give minimum d spacings of 31–32 Å for the same plasmid DNA as used in the present study¹⁵ and somewhat larger than would be expected for hydrated DNA (strand–strand repulsion prevents actual contact).

Factors Facilitating Formation of DNA-Coated Vesicles. As shown above, DNA-coated vesicles coexist with multilamellar lipoplexes when free DNA also coexists in solution. Since the D:L ratio was not less than 0.7 (plasmid DNA) under those conditions, a lipoid charge excess of at least $1.0/0.7 = 1.4$ is necessary for transformation of DNA-coated vesicles into multilamellar lipoplexes. Indeed, DNA-coated vesicles were observed to completely disappear after one hour of incubation if the lipoid charge exceeded the DNA charge by about 40%.

Several conditions were found to destabilize DNA-coated vesicles and to shift the distribution toward fused multilamellar lipoplexes. In particular, plasmid DNA rather than linear DNA, large multilamellar vesicles rather than small unilamellar vesicles, low concentrations ($\leq 10 \mu\text{M}$), and prolonged incubation times all favored multilamellar complexes relative to DNA-coated vesicles. These findings can be rationalized in terms of the mechanism of cationic lipoid–DNA complex formation presented here.

Flow Fluorometry Can Establish the Coexistence of Two Phases in the Same Particle. The behavior of another cationic lipoid, DOTAP, has been extensively studied by, among other methods, X-ray diffraction. It was found that when lipoplexes are formed from more than about a 3-fold excess of lipoid, the DNA strand spacing becomes constant.^{11,42} At such high excesses of lipoid, the preparation must therefore consist of two phases: one containing DNA and one devoid of DNA. Diffraction cannot distinguish whether the phases coexist in the same lipoplex particle or they are in separate particles. Although our diffraction studies on EDOPC have not included large lipoid excesses, so that we do not know whether an EDOPC phase separates from an EDOPC phase as in the case of DOTAP, it is nevertheless clear from flow fluorometry that a very large excess of EDOPC can be present in a single lipoplex particle for at least several hours.

Biological Implications of Lipoplex Preparation Heterogeneity. Typically, a small fraction of the total DNA actually reaches the cell nucleus in most lipofection procedures.⁴⁵ Does this mean that a small subpopulation is especially effective, or does it just reflect the low probability of lipofection? Information on the heterogeneity of lipoplexes is essential to answer this question. The heterogeneity comes from both liposome heterogeneity and their asymmetric structure, with accessible and inaccessible lipoid. Here, we have established two main contributors to lipoplex heterogeneity: DNA-coated vesicles and multilamellar lipoplex particles.

DNA-coated vesicles are likely to be ineffective in transfection because their external surface is anionic. This is supported by the typical finding (for cationic phospholipid derivatives related to EDOPC as well as for the many other cationic amphipaths commonly used for transfection) that for efficient lipofection some lipoid excess is typically necessary—the condition that not only gives rise to positive particles but also, as shown here, facilitates formation of multilamellar lipoplexes at the expense of DNA-coated vesicles. Given that multilamellar lipoplexes are desirable for transfection, the procedures described here allow preparing lipoplexes with the optimal size and even some control over the heterogeneity of the population.

Acknowledgment. This work was supported by NIH grants GM52329 and GM57305. We thank Robert A. Lamb for generously providing access to the flow cytometry instrument.

MP700080M